Combined Effects of Surface Energy, Initial Stress and Nonlocality on Vibration of Carbon Nanotubes Conveying Fluid Resting on Elastic Foundations in a Thermo-Magnetic Environment

Olasunkanmi A. Afolabi[1], Suraju A. Oladosu[2], Rafiu O. Kuku[3], Gbeminiyi Musibau Sobamowo[4], Ahmed A. Yinusa[5], Rilwan O. Olagbadamosi[6]

[1,2,3,6] Department of Mechanical Engineering, Lagos State University, Nigeria.
[4,5]Department of Mechanical Engineering, University of Lagos, Nigeria.

Corresponding author:
Gbeminiyi Musibau Sobamowo
University of Lagos, Nigeria
Email: mikegbeminiyiprof@yahoo.com

Abstract

This paper scrutinizes the simultaneous impacts of surface elasticity, initial stress, residual surface stress and nonlocality on the nonlinear vibration of carbon nanotube conveying fluid resting while resting on linear and nonlinear elastic foundations and operating in a thermo-magnetic environment. The equation for vibration of the structures after decomposition into spatial and temporal parts is solved by homotopy perturbation method. Parametric studies of the pertinent parameters of the model are carried out. The investigations show that the positive and negative surface stress abates and improves the frequency ratio, respectively. The surface effect and frequency ratio are reduced as the length of the structure and nonlocality increase while the magnetic field strength and the nonlocal parameter decreases as the frequency ratio is increases. At a high temperature, the frequency ratio is inversely proportional with the temperature change but directly proportional to the temperature change at room/low temperature. The work has provided good understanding on the vibration behaviour of the nanotube and therefore, it will be very useful in the design and control of structures.

Keywords: Surface effects, Carbon nanotubes, Nonlocal elasticity theory, Homotopy perturbation method.

INTRODUCTION

After the discovery of nanostructures discovered by Iijima [1], different studies on the utilizations of nanomaterials have showed the importance of carbon nanotubes (CNTs) for medical, industrial, electrical, thermal, electronic and mechanical applications [2-5]. Vibration of the nanostructures have been studied but the simultaneous effects of the surface energy and initial stress was not explored [6-13]. The effects of these parameters have been found to be very significant in the vibration analysis of the structures [13-20]. Therefore, Wang [13] presented a study where the effects of surface energy on the vibration of CNTs were analyzed. Zhang and Meguid [14] investigated the impacts of the surface energy on the vibration of nanobeams-carrying fluids. Hosseini et al. [15] explored the significance of such energy on the instability characteristics of cantilever piezoelectric CNTs carrying fluid while the influences of surface energy and nonlocality were explored by Bahaadini et al. [16]. Other researchers [17-28] have used different theories and method to examine the effects of surface stress and energy on the nanostructures.

The impacts of initial stress on the vibration of CNTs have been observed [29-37]. However, the combined effects of surface behaviours, nonlocality and initial stress on the physical characteristics and mechanical behaviours of CNTs have not been explored. Also, such studies have not been extended to vibration characteristics of CNTs resting of elastic foundations in a thermo-magnetic environment. Therefore, in this present study, the scrutinizes the simultaneous impacts of surface elasticity, initial stress, residual surface stress and nonlocality on the nonlinear vibration of carbon nanotube conveying fluid resting while resting on linear and nonlinear elastic foundations and operating in a thermo-magnetic environment. The equation for vibration of the structures after decomposition into spatial and temporal parts is solved by homotopy perturbation method. Parametric studies of the pertinent parameters of the model are carried out.

METHODS
Model Development

Consider a single-walled CNT of length L and outer and inner diameters Do and Di resting on Winkler (Spring) and Pasternak (Shear layer) foundations as illustrated in Figure 1. The figure illustrates SWCNTs carrying a hot fluid while resting on elastic foundations under magnetic field.
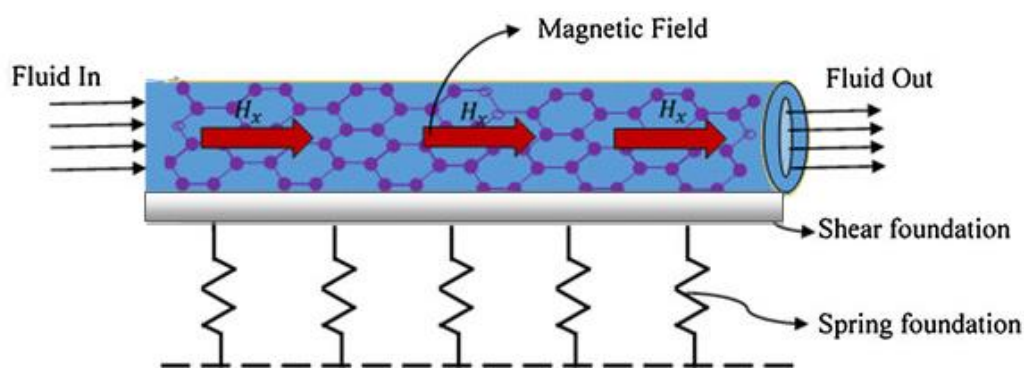

Figure 1. Carbon nanotube conveying hot fluid resting on elastic foundation

From Erigen's nonlocal elasticity [38-39], the differential relations for stress and strains for the CNTs is

$$\sigma_{xx} - \left(e_0 a\right)^2 \frac{\partial^2 \sigma_{xx}}{\partial x^2} = E \varepsilon_{xx} \tag{1}$$

The strain–displacement relation,

$$\varepsilon_{xx} = -z \frac{\partial^2 w(x,t)}{\partial x^2} \tag{2}$$

In case of small deformation, the strain–displacement relation

$$\varepsilon_{xx} = -z \frac{\partial^2 w}{\partial x^2} \tag{3}$$

Therefore,

$$\sigma_{xx} - \left(e_0 a\right)^2 \frac{\partial^2 \sigma_{xx}}{\partial x^2} = -Ez \frac{\partial^2 w}{\partial x^2} \tag{4}$$

Multiply Eq. (4) through by zdA

$$\sigma_{xx} z dA - \left(e_0 a\right)^2 \frac{\partial^2 \left(z \sigma_{xx}\right)}{\partial x^2} dA = -Ez^2 \frac{\partial^2 w}{\partial x^2} dA \tag{5}$$

On integrating both sides of Eq. (8), we have

$$\int_A \sigma_{xx} z dA - \left(e_0 a\right)^2 \frac{\partial^2}{\partial x^2} \int_A z \sigma_{xx} dA = -E \frac{\partial^2 w}{\partial x^2} \int_A z^2 dA \tag{6}$$

Recall that the bending moment and second moment of area (area moment of inertia) are given as

$$M = \int_A z \sigma_{xx} dA \tag{7}$$

and

$$I = \int_A z^2 dA \tag{8}$$

Therefore, Eq. (6) can be written as

$$M - \left(e_0 a\right)^2 \frac{\partial^2 M}{\partial x^2} = -EI \frac{\partial^2 w}{\partial x^2} \tag{9}$$

If Eq. (9) is differentiated twice, we have

$$\frac{\partial^2 M}{\partial x^2} - \left(e_0 a\right)^2 \frac{\partial^2}{\partial x^2} \left(\frac{\partial^2 M}{\partial x^2} \right) = -EI \frac{\partial^4 w}{\partial x^4} \tag{10}$$

Therefore,

$$EI \frac{\partial^4 w}{\partial x^4} + \frac{\partial^2 M}{\partial x^2} - (e_0 a)^2 \frac{\partial^2}{\partial x^2}\left(\frac{\partial^2 M}{\partial x^2}\right) = 0 \tag{11}$$

If the effect of surface is considered, we have

$$\left(EI + E_s I_s\right)\frac{\partial^4 w}{\partial x^4} + \frac{\partial^2 M}{\partial x^2} - (e_0 a)^2 \frac{\partial^2}{\partial x^2}\left(\frac{\partial^2 M}{\partial x^2}\right) = 0$$

(12)

From the Euler beam theory,

$$\frac{\partial^2 M}{\partial x^2} = m_{cn}\frac{\partial^2 w}{\partial t^2} + f_{fluid\ flow} - f_{initial\ stress} + f_{axial\ tension} + f_{residual\ surface\ stress} + f_{foundation} + f_{magnetic} - f_{thermal}$$

(13)

The above forces are per unit length,

The axial force due to flow of fluid

$$f_{fluid\ flow} = m_f \frac{\partial^2 w}{\partial t^2} + m_f u^2 \frac{\partial^2 w}{\partial x \partial t} + 2um_f \frac{\partial^2 w}{\partial x \partial t} \tag{14}$$

The axial force because of initial stress

$$f_{initial\ stress} = -\delta A \sigma_x^o \frac{\partial^2 w}{\partial x^2} \tag{15}$$

The axial force as a result of residual surface stress

$$f_{residual\ surface\ stress} = H_s \frac{\partial^2 w}{\partial x^2} \tag{16}$$

The axial force because of axial tension/support

$$f_{axial\ support} = \left[\frac{EA}{2L}\int_0^L \left(\frac{\partial w}{\partial x}\right)^2 dx\right]\frac{\partial^2 w}{\partial x^2} \tag{17}$$

The force from the Winkler and Pasternak foundations is given as

$$f_{foundation} = k_1 w - k_p \frac{\partial^2 w}{\partial x^2} + k_3 w^3 \tag{18}$$

The magnetic force as a result of Lorentz force.

$$f_{magnetic} = \eta H_x^2 A \frac{\partial^2 w}{\partial x^2} \tag{19}$$

The axial force due to thermal effect

$$f_{thermal} = -\frac{EA\alpha\Delta T}{1-2v}\frac{\partial^2 w}{\partial x^2} \tag{20}$$

Substituting Eqs. (14) – (20) into Eq. (13), we have

$$\frac{\partial^2 M}{\partial x^2} = (m_{cn} + m_f)\frac{\partial^2 w}{\partial t^2} + 2um_f\frac{\partial^2 w}{\partial x \partial t} + \left[\frac{EA}{2L}\int_0^L \left(\frac{\partial w}{\partial x}\right)^2 dx\right]\frac{\partial^2 w}{\partial x^2}$$

$$+\left(m_f u^2 + \delta A\sigma_x^o - H_s - \eta H_x^2 A - k_p + \frac{EA\alpha\Delta T}{1-2\nu}\right)\frac{\partial^2 w}{\partial x^2} + k_1 w + k_3 w^3 \tag{21}$$

On putting Eq. (20) into Eq. (12), we arrived at

$$\left(EI + E_s I_s\right)\frac{\partial^4 w}{\partial x^4} + (m_{cn} + m_f)\frac{\partial^2 w}{\partial t^2} + 2um_f\frac{\partial^2 w}{\partial x \partial t} + \left[\frac{EA}{2L}\int_0^L \left(\frac{\partial w}{\partial x}\right)^2 dx\right]\frac{\partial^2 w}{\partial x^2}$$

$$+\left(m_f u^2 + \delta A\sigma_x^o - H_s - \eta H_x^2 A - k_p + \frac{EA\alpha\Delta T}{1-2\nu}\right)\frac{\partial^2 w}{\partial x^2} + k_1 w + k_3 w^3$$

$$-\left(e_o a\right)^2 \left[\begin{array}{l} (m_{cn} + m_f)\frac{\partial^4 w}{\partial x^2 \partial t^2} + 2um_f\frac{\partial^4 w}{\partial x^3 \partial t} + \left[\frac{EA}{2L}\int_0^L \left(\frac{\partial w}{\partial x}\right)^2 dx\right]\frac{\partial^4 w}{\partial x^4} \\ +\left(m_f u^2 + \delta A\sigma_x^o - H_s - \eta H_x^2 A - k_p + \frac{EA\alpha\Delta T}{1-2\nu}\right)\frac{\partial^4 w}{\partial x^4} \\ +k_1 \frac{\partial^2 w}{\partial x^2} + 3k_3 w^2 \frac{\partial^2 w}{\partial x^2} + 6k_3 w\left(\frac{\partial w}{\partial x}\right)^2 \end{array}\right] = 0 \tag{22}$$
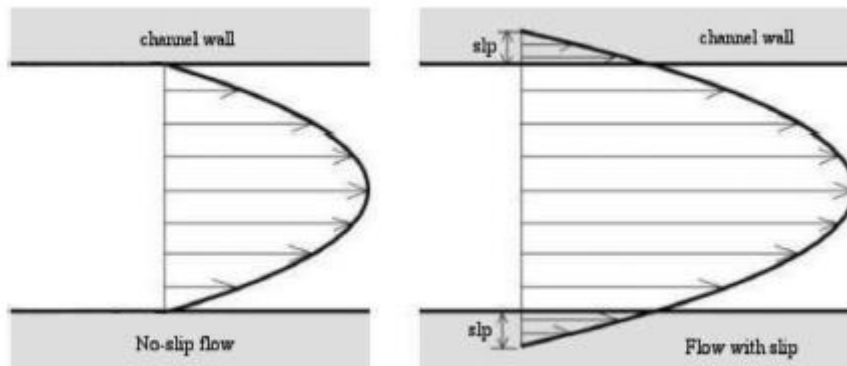

Figure 2. Effect of slip boundary condition on velocity profile [40, 41].

Figure 2 shows the effect of flow in a channel. In the fluid-conveying carbon nanotube, the condition of slip is satisfied since in such flow, the ratio of the mean free path of the fluid molecules relative to a characteristic length of the flow geometry which is the Knudsen number is larger than 10-2. Consequently, the velocity correction factor for the slip flow velocity is proposed as [40, 41]:

$$VCF = \frac{u_{avg,slip}}{u_{avg,no-slip}} = \left(1 + a_k Kn\right)\left[4\left(\frac{2-\sigma_v}{\sigma_v}\right)\left(\frac{Kn}{1+Kn}\right)+1\right] \tag{23}$$

Where in practice, $\sigma_v = 0.7$ [40, 41]

$$a_k = a_o \frac{2}{\pi}\left[tan^{-1}\left(a_1 Kn^B\right)\right] \tag{24}$$

$$a_o = \frac{64}{3\pi\left(1-\frac{4}{b}\right)} \tag{25}$$

$a_1 = 4$, $b = -1$ and B = 0.04. Where b is the general slip coefficient

From Eq. (23),

$$u_{avg,slip} = \left(1 + a_k Kn\right)\left[4\left(\frac{2-\sigma_v}{\sigma_v}\right)\left(\frac{Kn}{1+Kn}\right)+1\right]u_{avg,no-slip} \tag{26}$$

Therefore, Eq. (22) can be written as

$$\left(EI + E_s I_s\right)\frac{\partial^4 w}{\partial x^4} + (m_{cn} + m_f)\frac{\partial^2 w}{\partial t^2} + 2m_f\left(1+a_k Kn\right)\left[4\left(\frac{2-\sigma_v}{\sigma_v}\right)\left(\frac{Kn}{1+Kn}\right)+1\right]\frac{\partial^2 w}{\partial x \partial t} + \left[\frac{EA}{2L}\int_0^L\left(\frac{\partial w}{\partial x}\right)^2 dx\right]\frac{\partial^2 w}{\partial x^2}$$

$$+ \left(m_f\left[\left(1+a_k Kn\right)\left[4\left(\frac{2-\sigma_v}{\sigma_v}\right)\left(\frac{Kn}{1+Kn}\right)+1\right]\right]^2 + \delta A\sigma_x^o - H_s - \eta H_x^2 A - k_p + \frac{EA\alpha\Delta T}{1-2\nu}\right)\frac{\partial^2 w}{\partial x^2} + k_1 w + k_3 w^3$$

$$-(e_o a)^2\left[\begin{array}{l}(m_{cn}+m_f)\dfrac{\partial^4 w}{\partial x^2 \partial t^2} + 2m_f\left(1+a_k Kn\right)\left[4\left(\dfrac{2-\sigma_v}{\sigma_v}\right)\left(\dfrac{Kn}{1+Kn}\right)+1\right]\dfrac{\partial^4 w}{\partial x^3 \partial t} + \left[\dfrac{EA}{2L}\int_0^L\left(\dfrac{\partial w}{\partial x}\right)^2 dx\right]\dfrac{\partial^4 w}{\partial x^4} \\[4mm] + \left(m_f\left[\left(1+a_k Kn\right)\left[4\left(\dfrac{2-\sigma_v}{\sigma_v}\right)\left(\dfrac{Kn}{1+Kn}\right)+1\right]\right]^2 + \delta A\sigma_x^o - H_s - \eta H_x^2 A - k_p + \dfrac{EA\alpha\Delta T}{1-2\nu}\right)\dfrac{\partial^4 w}{\partial x^4} \\[4mm] + k_1\dfrac{\partial^2 w}{\partial x^2} + 3k_3 w^2\dfrac{\partial^2 w}{\partial x^2} + 6k_3 w\left(\dfrac{\partial w}{\partial x}\right)^2\end{array}\right] = 0$$

$$\tag{27}$$

where the transverse area and the bending rigidity are given as

$$A = \pi d h$$

$$EI = \frac{\pi d^3 h}{8}$$

and

$$E_s I_s = \frac{\pi E_s h(d_o^3 + d_i^3)}{8}$$

$$H_s = 2\tau_s\left(d_o + d_i\right)$$

The symbol H_s is the parameter induced by residual surface stress, τ is residual surface tension, d and h are the nanotube internal diameter and thickness, respectively. It should be noted that the diameter of the nanotube can be developed from chirality indices (n, m).

$$d_i = \frac{a\sqrt{3}}{\pi}\sqrt{n^2 + mn + m^2} \tag{28}$$

where $a\sqrt{3} = 0.246\,nm$. "a" represents the length of the carbon-carbon bond. d is the inner diameter of the nanotube.

Analytical Solutions of Nonlinear Model of Free Vibration of the nanotube

The nonlinear term in model in Eq. (27) makes it very difficult to provide closed-form solution to the problem. Therefore, recourse is made to homotopy perturbation to solve the nonlinear model. In order to develop analytical solutions for the developed nonlinear model, the partial differential equation is converted to ordinary differential equation using the Galerkin's decomposition procedure to decompose the spatial and temporal parts of the lateral displacement functions as

$$w(x,t) = \phi(x)u(t) \qquad (29)$$

Where $u(t)$ the generalized coordinate of the system and $\phi(x)$ is a trial/comparison function that will satisfy both the geometric and natural boundary conditions.

Applying one-parameter Galerkin's solution given in Eq. (29) to Eq. (27)

$$\int_0^L R(x,t)\phi(x)dx \qquad (30)$$

where

$$R(x,t) = \left(EI + E_s I_s\right)\frac{\partial^4 w}{\partial x^4} + (m_{cn} + m_f)\frac{\partial^2 w}{\partial t^2} + 2m_f\left(1 + a_k Kn\right)\left[4\left(\frac{2-\sigma_v}{\sigma_v}\right)\left(\frac{Kn}{1+Kn}\right)+1\right]\frac{\partial^2 w}{\partial x \partial t} + \left[\frac{EA}{2L}\int_0^L\left(\frac{\partial w}{\partial x}\right)^2 dx\right]\frac{\partial^2 w}{\partial x^2}$$

$$+ \left(m_f\left[\left(1+a_k Kn\right)\left[4\left(\frac{2-\sigma_v}{\sigma_v}\right)\left(\frac{Kn}{1+Kn}\right)+1\right]\right]^2 + \delta A\sigma_x^o - H_s - \eta H_x^2 A - k_p + \frac{EA\alpha\Delta T}{1-2v}\right)\frac{\partial^2 w}{\partial x^2} + k_1 w + k_3 w^3$$

$$-(e_o a)^2\left[\begin{array}{c}(m_{cn}+m_f)\dfrac{\partial^4 w}{\partial x^2 \partial t^2} + 2m_f\left(1+a_k Kn\right)\left[4\left(\dfrac{2-\sigma_v}{\sigma_v}\right)\left(\dfrac{Kn}{1+Kn}\right)+1\right]\dfrac{\partial^4 w}{\partial x^3 \partial t} + \left[\dfrac{EA}{2L}\int_0^L\left(\dfrac{\partial w}{\partial x}\right)^2 dx\right]\dfrac{\partial^4 w}{\partial x^4} \\[2mm] + \left(m_f\left[\left(1+a_k Kn\right)\left[4\left(\dfrac{2-\sigma_v}{\sigma_v}\right)\left(\dfrac{Kn}{1+Kn}\right)+1\right]\right]^2 + \delta A\sigma_x^o - H_s - \eta H_x^2 A - k_p + \dfrac{EA\alpha\Delta T}{1-2v}\right)\dfrac{\partial^4 w}{\partial x^4} \\[2mm] + k_1\dfrac{\partial^2 w}{\partial x^2} + 3k_3 w^2\dfrac{\partial^2 w}{\partial x^2} + 6k_3 w\left(\dfrac{\partial w}{\partial x}\right)^2\end{array}\right] = 0$$

We have the nonlinear vibration equation of the pipe as

$$M\ddot{u}(t) + G\dot{u}(t) + (K+C)u(t) + Vu^3(t) = 0 \qquad (31)$$

where

$$M = (m_p + m_f)\left[\int_0^L \phi^2(x)dx - \left(e_o a\right)^2 \int_0^L \phi^2(x)\frac{d^2\phi}{dx^2}dx\right]$$

$$G = \left[2m_f\left(1+a_k Kn\right)\left[4\left(\frac{2-\sigma_v}{\sigma_v}\right)\left(\frac{Kn}{1+Kn}\right)+1\right]\right]\int_0^L\left[\phi(x)\left(\frac{d\phi}{dx}\right)dx - \left(e_o a\right)^2 \int_0^L \phi(x)\frac{d^3\phi}{dx^3}dx\right]$$

$$K = \int_0^L \left(EI + E_s I_s \right) \phi(x) \frac{d^4\phi}{dx^4} dx + k_1 \left[\int_0^L \phi^2(x) dx - \left(e_o a \right)^2 \int_0^L \phi(x) \frac{d^2\phi}{dx^2} dx \right]$$

$$C = \left(\begin{array}{c} m_f \left[\left(1 + a_k Kn \right) \left[4 \left(\frac{2-\sigma_v}{\sigma_v} \right) \left(\frac{Kn}{1+Kn} \right) + 1 \right] \right]^2 \\ + \delta A \sigma_x^o - H_s - \eta H_x^2 A - k_p + \frac{EA\alpha\Delta T}{1-2\nu} \end{array} \right) \left[\int_0^L \phi(x) \frac{d^2\phi}{dx^2} dx - \left(e_o a \right)^2 \int_0^L \phi(x) \frac{d^4\phi}{dx^4} dx \right]$$

$$V = k_3 \left[\int_0^L \phi^4(x) dx - \left(e_o a \right)^2 \left(3 \int_0^L \phi^3(x) \frac{d^2\phi}{dx^2} dx + 6 \int_0^L \phi^2(x) \left(\frac{d\phi}{dx} \right)^2 dx \right) \right]$$

$$+ \int_0^L \phi(x) \left[\frac{EA}{2L} \int_0^L \left(\frac{d\phi}{dx} \right)^2 dx \right] \frac{d^2\phi}{dx^2} dx - \left(e_o a \right)^2 \int_0^L \phi(x) \left[\frac{EA}{2L} \int_0^L \left(\frac{d\phi}{dx} \right)^2 dx \right] \frac{d^4\phi}{dx^4} dx$$

The circular fundamental natural frequency gives

$$\omega_n = \sqrt{\frac{K+C}{M}} \qquad (32)$$

For the simply supported pipe,

$$\phi(x) = \sin\beta_n x \qquad (33)$$

where

$$\sin\beta L = 0 \quad \Rightarrow \beta_n = \frac{n\pi}{L}$$

Eq. (33) can be written as

$$\ddot{u}(t) + \gamma\dot{u}(t) + \alpha u(t) + \beta u^3(t) = 0 \qquad (34)$$

where

$$\alpha = \frac{(K+C)}{M}, \quad \beta = \frac{V}{M}, \quad \gamma = \frac{G}{M},$$

For an undamped simple-simple supported structures, where *G = 0,* we have

$$\ddot{u}(t) + \alpha u(t) + \beta u^3(t) = 0 \qquad (35)$$

More on the principle of the decomposition can be found in our previous study [42].

Homotopy perturbation method

Homotopy perturbation methos is a total analytical power series method for solving nonlinear equations. It is first proposed by He [43]. The method was also improved by He [44-47]. Its basic principle is stated in the next section.

The basic idea of homotopy perturbation method

In order to establish the basic idea behind homotopy perturbation method, consider a system of nonlinear differential equations given as

$$A(U) - f(r) = 0, \quad r \in \Omega, \tag{36}$$

with the boundary conditions

$$B\left(u, \frac{\partial u}{\partial \eta}\right) = 0, \qquad r \in \Gamma, \tag{37}$$

where A is a general differential operator, B is a boundary operator, $f(r)$ a known analytical function and Γ is the boundary of the domain Ω.

The operator A can be decomposed or divided into two parts, which are L and N, where L is a linear operator, N is a non-linear operator. Eq. (36) can be therefore rewritten as follows

$$L(u) + N(u) - f(r) = 0. \tag{38}$$

By the homotopy technique, a homotopy $U(r, p) : \Omega \times [0,1] \to R$ can be constructed, which satisfies

$$H(U, p) = (1 - p)\left[L(U) - L(U_o)\right] + p\left[A(U) - f(r)\right] = 0, \quad p \in [0,1], \tag{39}$$

or

$$H(U, p) = L(U) - L(U_o) + pL(U_o) + p\left[N(U) - f(r)\right] = 0. \tag{40}$$

In the above Eqs. (39) and (40), $p \in [0,1]$ is an embedding parameter, u_o is an initial approximation of equation of Eq.(36), which satisfies the boundary conditions.

Also, from Eqs. (39) and Eq. (40), we will have

$$H(U, 0) = L(U) - L(U_o) = 0, \tag{41}$$

or

$$H(U, 1) = A(U) - f(r) = 0. \tag{42}$$

The changing process of p from zero to unity is just that of $U(r, p)$ from $u_o(r)$ to $u(r)$. This is referred to deformation in topology. $L(U) - L(U_o)$ and $A(U) - f(r)$ are called homotopic.

Using the embedding parameter p as a small parameter, the solution of Eqs. (39) and Eq. (40) can be assumed to be written as a power series in p as given in Eq. (43)

$$U = U_o + pU_1 + p^2 U_2 + \dots \tag{43}$$

It should be pointed out that of all the values of p between 0 and 1, *p=1* produces the best result. Therefore, setting $p = 1$, results in the approximation solution of Eq. (44)

$$u = \lim_{p \to 1} U = U_o + U_1 + U_2 + \dots \tag{44}$$

Therefore

$$u = U_o + U_1 + U_2 + \dots \tag{45}$$

The series Eq. (45) is convergent for most cases.

The basic idea expressed above is a combination of homotopy and perturbation method. Hence, the method is called homotopy perturbation method (HPM), which has eliminated the limitations of the traditional perturbation methods. On the other hand, this technique can have full advantages of the traditional perturbation techniques.

Homotopy Perturbation Method to the Nonlinear Vibration Problem

The nonlinear model is solved in this section using homotopy perturbation method (HPM). The approximate analytical method provides total analytical procedures and solutions to the developed nonlinear model.

Using HPM, one can write an homotopy for Eq. (35) as

$$H(u,p) = (1-p)[\ddot{u} + \alpha u] + p[\ddot{u} + \alpha u + \beta u^3] = 0, \quad p \in [0,1] \tag{46}$$

Or equivalently,

$$H(u,p) = \ddot{u} + \alpha u + p[\beta u^3] = 0, \quad p \in [0,1] \tag{47}$$

Taking the solution of Eq. (44) to be expressed in a series as:

$$u = u_0 + pu_1 + p^2 u_2 + p^3 u_3 + \ldots \tag{48}$$

Also, the constant α can be expanded as

$$\alpha = \omega_0^2 + p\omega_1^2 + p^2 \omega_2^2 + p^3 \omega_2^3 + \ldots \tag{49}$$

Putting Eqs. (48) and (49) into Eq.(47), gives

$$\left(\ddot{u}_0 + p\ddot{u}_1 + p^2 \ddot{u}_2 + p^3 \ddot{u}_3 + \ldots\right) + \left(\omega_0^2 + p\omega_1^2 + p^2 \omega_2^2 + p^3 \omega_3^2 + \ldots\right)\left(u_0 + pu_1 + p^2 u_2 + p^3 u_3 + \ldots\right) +$$
$$p\beta\left(u_0 + pu_1 + p^2 u_2 + p^3 u_3 + \ldots\right)^3 = 0$$

$$\tag{50}$$

From Eq. (50), one can deduce that

$$p^0: \quad \ddot{u} + \omega_0^2 u_0 = 0 \tag{51}$$

$$p^1: \quad \ddot{u}_1 + \omega_0^2 u_1 + \omega_2^2 u_0 + \beta u_0^3 = 0 \tag{52}$$

$$p^2: \quad \ddot{u}_2 + \omega_0^2 u_2 + \omega_1^2 u_1 + \omega_2^2 u_0 + 3\beta u_0^2 u_1 = 0 \tag{53}$$

$$p^3: \ddot{u}_3 + \omega^2 u_3 + \omega_0^2 u_3 + \omega_1^2 u_2 + \omega_2^2 u_0 + 2\beta\left(u_0^2 u_2 + u_1^2 u_0\right) = 0 \tag{54}$$

the initial conditions for the above equations are:

$$u_0(0) = A, \quad \dot{u}_0(0) = 0, \quad u_i(0) = 0, \quad \dot{u}_i(0) = 0, \quad (i = 1, 2, \ldots) \tag{55}$$

On solving Eq. (51) one can easily obtain

$$u_0 = A cos\omega_0 t \tag{56}$$

When the solution of u_0 in Eq. (56) into Eq.(52), we have

$$\ddot{u}_1 + \omega_0^2 u_1 + \left(\omega_1^2 A + \frac{3A^3\beta}{4} \right) cos\omega_0 t + \frac{A^3\beta}{4} cos3\omega_0 t = 0 \tag{57}$$

When the secular term in Eq. (52) is eliminated, one arrives at

$$\omega_1^2 = -\frac{3A^2\beta}{4} \tag{58}$$

And the solution of Eq. (57) under the initial conditions of Eq. (55) becomes

$$u_1 = \frac{A^3\beta}{32\omega_0^2} \left(cos3\omega_0 t - cos\omega_0 t \right) \tag{59}$$

Putting the solution in Eqs.(56) and (59) into Eq.(53), one arrives at

$$\ddot{u}_2 + \omega_0^2 u_2 + \left(a\omega_2^2 - \frac{3A^5\beta^2}{64\omega_0^2} - \frac{A^3\beta\omega_1^2}{32\omega_0^2} \right) cos\omega_0 t$$
$$+ \left(\frac{A^3\beta\omega_1^2}{32\omega_0^2} + \frac{3A^5\beta^2}{128\omega_0^2} \right) cos3\omega_0 t + \frac{3A^5\beta^2}{128\omega_0^2} cos5\omega_0 t = 0 \tag{60}$$

On eliminating the secular term in Eq. (60), we have

$$\omega_2^2 = \frac{3A^4\beta^2}{64\omega_0^2} + \frac{A^2\beta\omega_1^2}{32\omega_0^2} \tag{61}$$

Substituting Eq. (58) into Eq. (61), produces

$$\omega_2^2 = \frac{3A^4\beta^2}{128\omega_0^2} \tag{62}$$

Also, the solution of Eq. (60) under the initial conditions of Eq. (55) is

$$u_2 = \frac{A^5\beta^2}{1024\omega_0^4} \left(cos5\omega_0 t - cos\omega_0 t \right) \tag{63}$$

From Eqs. (50), (51) and (58), for the the first-order approximate solution, when $p=1$, we have

$$\omega_{0,1th} = \omega_0 = \sqrt{\alpha - \omega_1^2} = \sqrt{\alpha + \frac{3A^2\beta}{4}} \tag{64}$$

and

$$u_{1th} = A cos\omega_0 t + \frac{A^3\beta}{32\omega_0^2} \left(cos3\omega_0 t - cos\omega_0 t \right) \tag{65}$$

For the second-order approximate solution, when $p = 1$, from Eqs. (50), (51) and (58), we have

$$\omega_{0,2th} = \omega_0 = \frac{\sqrt{2}}{2}\sqrt{\alpha + \frac{3A^2\beta}{4} - \sqrt{\left(\alpha + \frac{3A^2\beta}{4}\right)^2 - \frac{3A^4\beta^2}{32}}} \qquad (66)$$

and

$$u_{2th} = \left(A - \frac{A^3\beta}{32\omega_0^2} - \frac{A^3\beta^2}{1024\omega_0^4}\right)cos\omega_0 t + \frac{A^3\beta}{32\omega_0^2}cos3\omega_0 t + \frac{A^5\beta^2}{1024\omega_0^4}cos5\omega_0 t \qquad (67)$$

Alternatively, if we substitute Eqs. (56), (59) and (63) into Eq. (50), we have

$$u = Acos\omega_0 t + p\left[\frac{A^3\beta}{32\omega_0^2}\left(cos3\omega_0 t - \cos\omega_0 t\right)\right] + p^2\left[\frac{A^5\beta^2}{1024\omega_0^4}\left(cos5\omega_0 t - cos\omega_0 t\right)\right] + ... \qquad (68)$$

For $p = 1$, the approximation solution of Eq.(68) is

$$u(t) = \left(A - \frac{A^3\beta}{32\omega_0^2} - \frac{A^5\beta^2}{1024\omega_0^4}\right)cos\omega_0 t + \frac{A^3\beta}{32\omega_0^2}cos3\omega_0 t + \frac{A^5\beta^2}{1024\omega_0^4}cos5\omega_0 t + ... \qquad (69)$$

Putting Eqs. (33) and (69) into Eq. (29), we have,

$$w(x,t) = \left\{\left(A - \frac{A^3\beta}{32\omega_0^2} - \frac{A^5\beta^2}{1024\omega_0^4}\right)cos\omega_0 t + \frac{A^3\beta}{32\omega_0^2}cos3\omega_0 t + \frac{A^5\beta^2}{1024\omega_0^4}cos5\omega_0 t + ...\right\}sin\frac{n\pi x}{L} \qquad (70)$$

where

$$\omega_0 = \frac{\sqrt{2}}{2}\sqrt{\alpha + \frac{3A^2\beta}{4} - \sqrt{\left(\alpha + \frac{3A^2\beta}{4}\right)^2 - \frac{3A^4\beta^2}{32}}} \qquad (71)$$

Therefore,

$$w(x,t) = \left\{\begin{array}{l}\left(A - \dfrac{A^3\beta}{16\left(\alpha + \frac{3A^2\beta}{4} - \sqrt{\left(\alpha + \frac{3A^2\beta}{4}\right)^2 - \frac{3A^4\beta^2}{32}}\right)} - \dfrac{A^5\beta^2}{256\left(\alpha + \frac{3A^2\beta}{4} - \sqrt{\left(\alpha + \frac{3A^2\beta}{4}\right)^2 - \frac{3A^4\beta^2}{32}}\right)^2}\right)cos\left(\frac{\sqrt{2}}{2}\sqrt{\alpha + \frac{3A^2\beta}{4} - \sqrt{\left(\alpha + \frac{3A^2\beta}{4}\right)^2 - \frac{3A^4\beta^2}{32}}}\,t\right) \\[2em] + \dfrac{A^3\beta}{16\left(\alpha + \frac{3A^2\beta}{4} - \sqrt{\left(\alpha + \frac{3A^2\beta}{4}\right)^2 - \frac{3A^4\beta^2}{32}}\right)}cos3\left(\frac{\sqrt{2}}{2}\sqrt{\alpha + \frac{3A^2\beta}{4} - \sqrt{\left(\alpha + \frac{3A^2\beta}{4}\right)^2 - \frac{3A^4\beta^2}{32}}}\,t\right) \\[2em] + \dfrac{A^5\beta^2}{256\left(\alpha + \frac{3A^2\beta}{4} - \sqrt{\left(\alpha + \frac{3A^2\beta}{4}\right)^2 - \frac{3A^4\beta^2}{32}}\right)^2}cos5\left(\frac{\sqrt{2}}{2}\sqrt{\alpha + \frac{3A^2\beta}{4} - \sqrt{\left(\alpha + \frac{3A^2\beta}{4}\right)^2 - \frac{3A^4\beta^2}{32}}}\,t + ...\right)\end{array}\right\}sin\frac{n\pi x}{L}$$

$$(72)$$

If the damped system is considered, the solutions of the first-order and the second-order frequency ratio are

$$\omega_{0,1th} = \sqrt{\alpha + \frac{3A^2\beta}{4}} \tag{73}$$

and

$$\omega_{0,2th} = \left[2\left(1 + \frac{3A^2\beta}{4\alpha}\right) - \left(\frac{\gamma^2}{\alpha^2}\right) \right] \pm \sqrt{\left[2\left(1 + \frac{3A^2\beta}{4\alpha}\right) - \left(\frac{\gamma^2}{\alpha^2}\right) \right]^2 - 4\left(1 + \frac{3A^2\beta}{4\alpha}\right)^2} \tag{74}$$

Alternatively,

$$\omega_{0,2th} = \sqrt{\alpha + \frac{3A^2\beta}{4} \pm \sqrt{\frac{1}{A^2} - \lambda^2\left(\alpha + \frac{3A^2\beta}{4}\right)}} \tag{75}$$

On substituting Eq. (74) into Eq. (70), we have

$$w(x,t) = \left\{ \begin{array}{l} \left[A - \dfrac{A^3\beta}{32\left\{\left[2\left(1+\frac{3A^2\beta}{4\alpha}\right)-\left(\frac{\gamma^2}{\alpha^2}\right)\right]\pm\sqrt{\left[2\left(1+\frac{3A^2\beta}{4\alpha}\right)-\left(\frac{\gamma^2}{\alpha^2}\right)\right]^2-4\left(1+\frac{3A^2\beta}{4\alpha}\right)^2}\right\}^2} \right. \\[2em] \left. - \dfrac{A^5\beta^2}{1024\left\{\left[2\left(1+\frac{3A^2\beta}{4\alpha}\right)-\left(\frac{\gamma^2}{\alpha^2}\right)\right]\pm\sqrt{\left[2\left(1+\frac{3A^2\beta}{4\alpha}\right)-\left(\frac{\gamma^2}{\alpha^2}\right)\right]^2-4\left(1+\frac{3A^2\beta}{4\alpha}\right)^2}\right\}^4} \right] cos\left\{\left\{\left[2\left(1+\frac{3A^2\beta}{4\alpha}\right)-\left(\frac{\gamma^2}{\alpha^2}\right)\right]\pm\sqrt{\left[2\left(1+\frac{3A^2\beta}{4\alpha}\right)-\left(\frac{\gamma^2}{\alpha^2}\right)\right]^2-4\left(1+\frac{3A^2\beta}{4\alpha}\right)^2}\right\}^2\right\}t \\[2em] + \dfrac{A^3\beta}{32\left\{\left[2\left(1+\frac{3A^2\beta}{4\alpha}\right)-\left(\frac{\gamma^2}{\alpha^2}\right)\right]\pm\sqrt{\left[2\left(1+\frac{3A^2\beta}{4\alpha}\right)-\left(\frac{\gamma^2}{\alpha^2}\right)\right]^2-4\left(1+\frac{3A^2\beta}{4\alpha}\right)^2}\right\}^2} cos3\left\{\left\{\left[2\left(1+\frac{3A^2\beta}{4\alpha}\right)-\left(\frac{\gamma^2}{\alpha^2}\right)\right]\pm\sqrt{\left[2\left(1+\frac{3A^2\beta}{4\alpha}\right)-\left(\frac{\gamma^2}{\alpha^2}\right)\right]^2-4\left(1+\frac{3A^2\beta}{4\alpha}\right)^2}\right\}^2\right\}t \\[2em] + \dfrac{A^5\beta^2}{1024\left\{\left[2\left(1+\frac{3A^2\beta}{4\alpha}\right)-\left(\frac{\gamma^2}{\alpha^2}\right)\right]\pm\sqrt{\left[2\left(1+\frac{3A^2\beta}{4\alpha}\right)-\left(\frac{\gamma^2}{\alpha^2}\right)\right]^2-4\left(1+\frac{3A^2\beta}{4\alpha}\right)^2}\right\}^4} cos5\left\{\left\{\left[2\left(1+\frac{3A^2\beta}{4\alpha}\right)-\left(\frac{\gamma^2}{\alpha^2}\right)\right]\pm\sqrt{\left[2\left(1+\frac{3A^2\beta}{4\alpha}\right)-\left(\frac{\gamma^2}{\alpha^2}\right)\right]^2-4\left(1+\frac{3A^2\beta}{4\alpha}\right)^2}\right\}^2\right\}t + ... \end{array} \right\} sin\frac{n\pi x}{L} \tag{76}$$

RESULTS AND DISCUSSION

The results of the simulations are given in Figures 3-12. While Figure 3 illustrates the verification of the present solution with the numerical solution using finite difference method (FDM), the significance of the model parameters on the vibration of CNTs are displayed in Figures 4-14.

Figure 4 illustrates the importance of the residual stress on the vibration characteristics of the CNTs. It is presented that the dynamic response of the CNTs different for negative and positive values of the residual stress. This establishes that the dynamic behaviour of the fluid-carrying CNTs is sensitive to the sign of the residual stress. Indisputably, as it is illustrated in the figure that at any given adimensional amplitude, there is an increase in the frequency ratio when the negative value of the surface stress increases while the ratio of the frequencies is lessened when the positive value of the stress is augmented because the negative values of stress reduce the linear stiffness of the nanostructure while the positive values of stress enhance the linear stiffness of the CNTs.

Figure 5 displays the significance of the stress, nonlocality and CNTs length on the ratio of the frequencies of the structure. The figures illustrates that the frequency ratio reduces when the CNTs length and thickness ratio are enhanced. It could also be stated that nonlocal parameter reduces the influences of the energy and stress at the surface on the frequency ratio. The results also display that the vibration frequency of the CNTs considering surface energy and stress is larger than the vibration frequency of the CNTs

given by the classical beam theory which does not consider the effect of surface energy and stress. Also, the figures present a clear statement that when the CNTs length is enlarged, the natural frequency of the nanotube gradually approaches the nonlinear Euler–Bernoulli beam limit due to reduction in the surface effect. Therefore, high
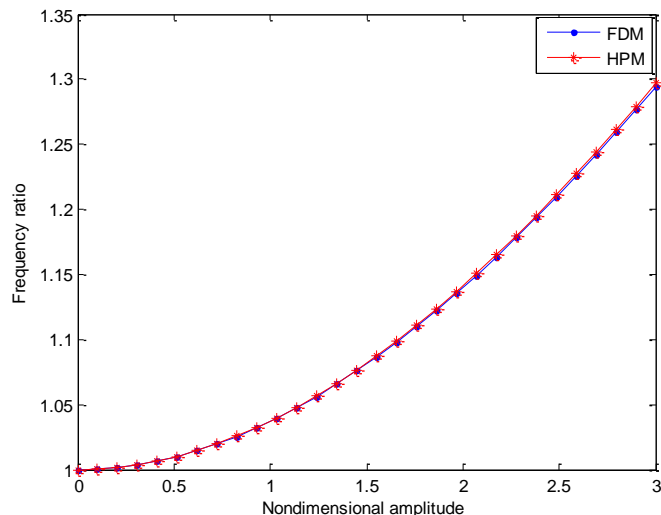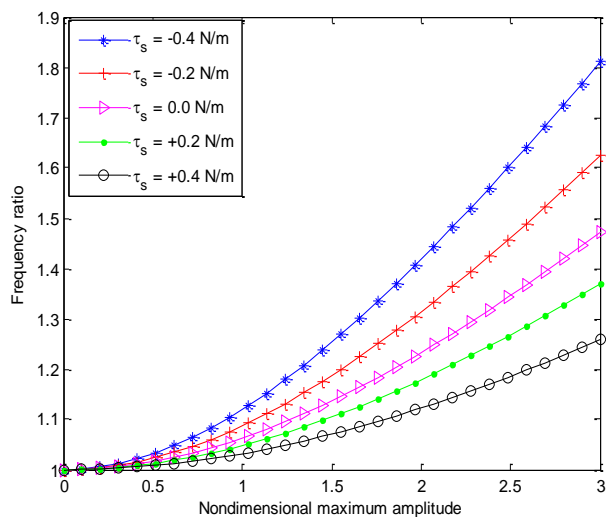

Figure 3. Comparison of HPM and FDM

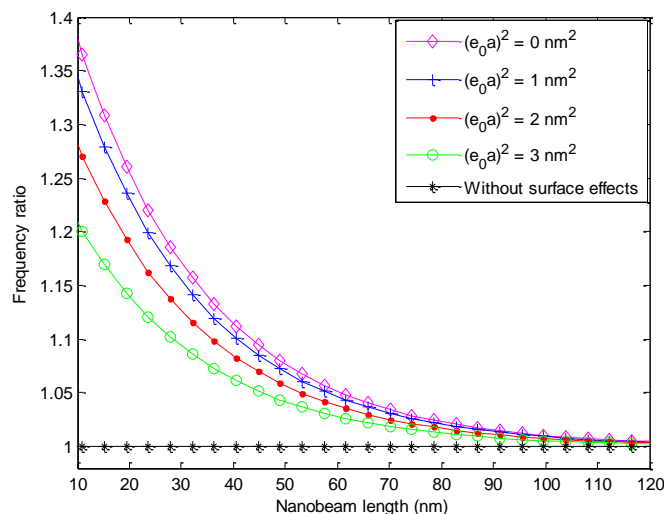**Figure 4.** Frequency ratio vs amplitude for difference residual stresses

Figure 5. Frequency ratio vs CNTs length for difference nonlocality parameters
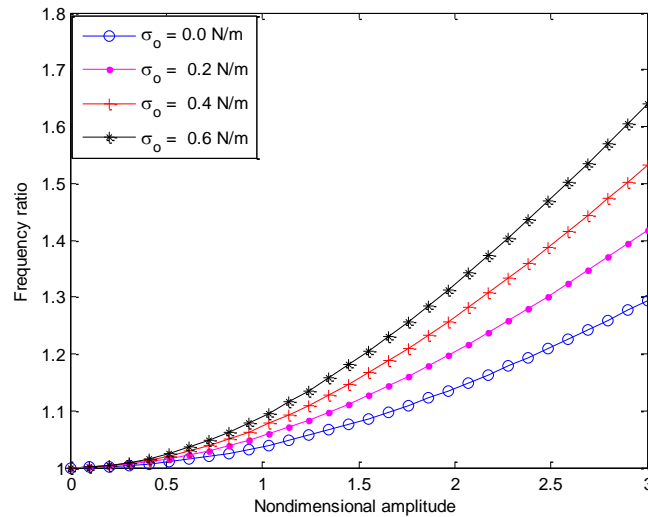
Figure 6. Frequency ratio vs amplitude for difference initial stresses
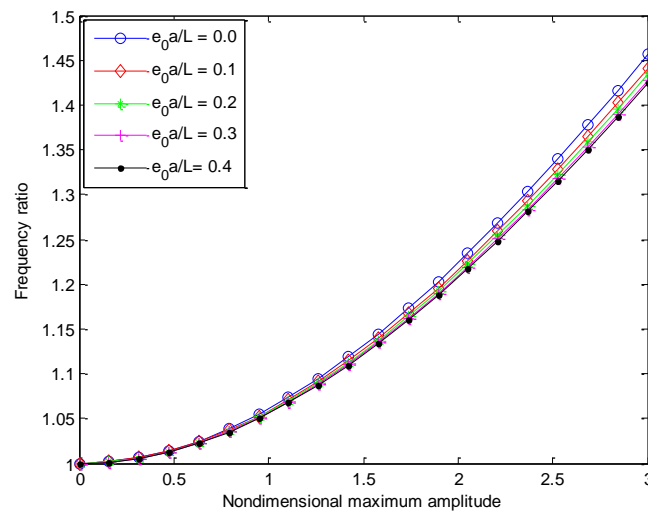
Figure 7. Frequency ratio vs amplitude for difference nonlocality parameters
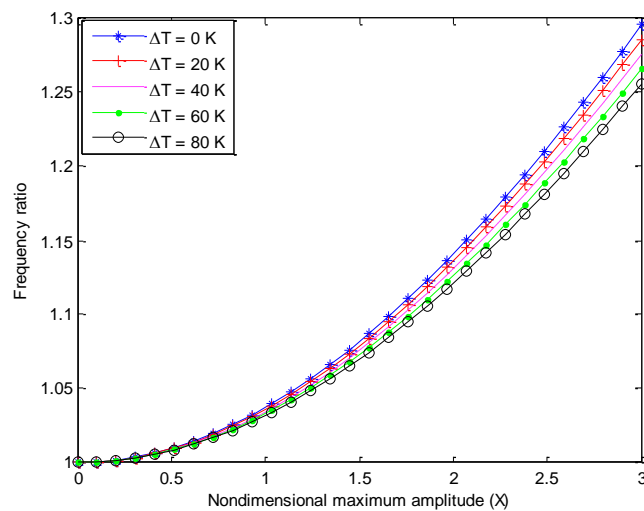

Figure 8. Frequency ratio vs amplitude for difference temperature change at high temperature

thickness ratios and long nanotube length make the impacts of the energy and stresses at the surface on the frequency ratio to vanish.
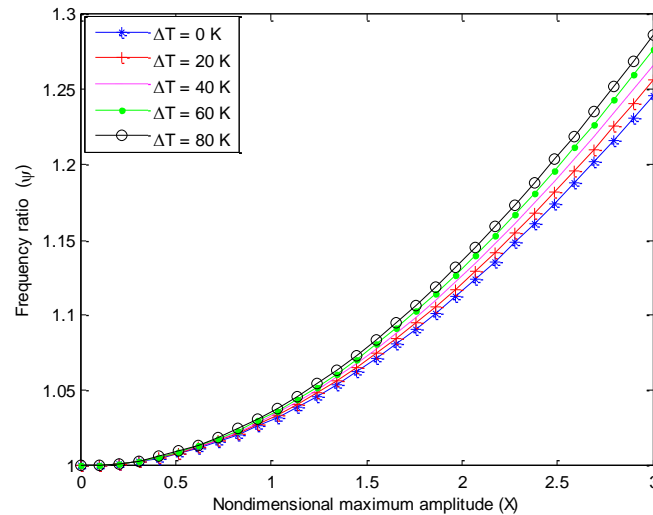
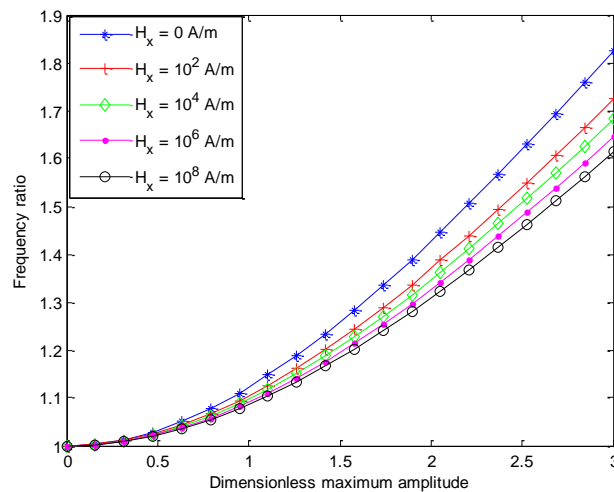**Figure 9**. Frequency ratio vs amplitude for difference temperature change at low temperature

Figure 10. Frequency ratio vs amplitude for difference magnetic field
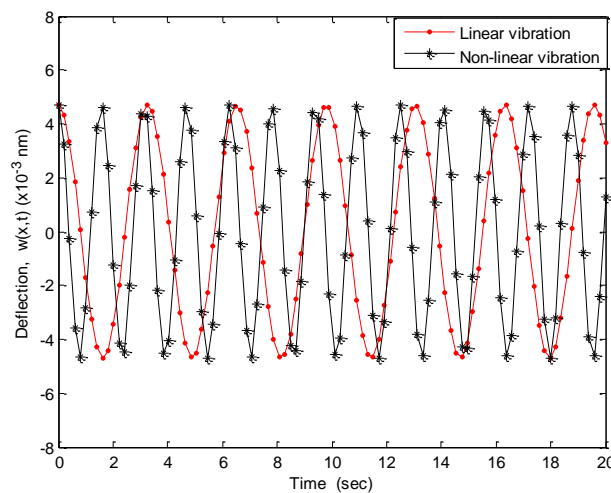

Figure 11. Linear and nonlinear dynamic behaviour of the nanostructure

Figure 6 analyzes the significance of initial stress on the vibration of the CNTs. It is depicted at any adimensional amplitude and initial stress increases, there is an enhancement in the ratio of the frequencies.
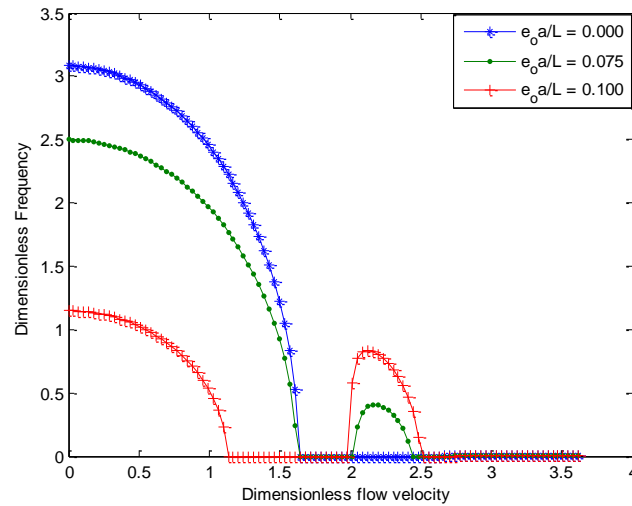
Figure 12. Nonlocality and fluid flow velocity impacts on the natural frequency of the CNTs
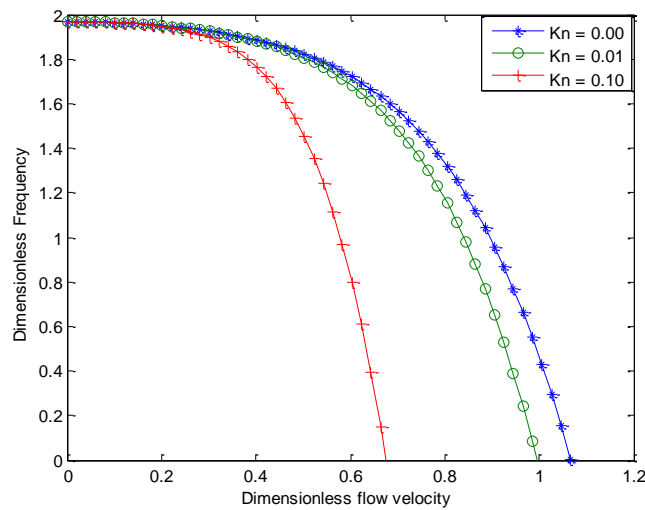

Figure 13. Slip and fluid flow velocity impacts on the natural frequency of the CNTs
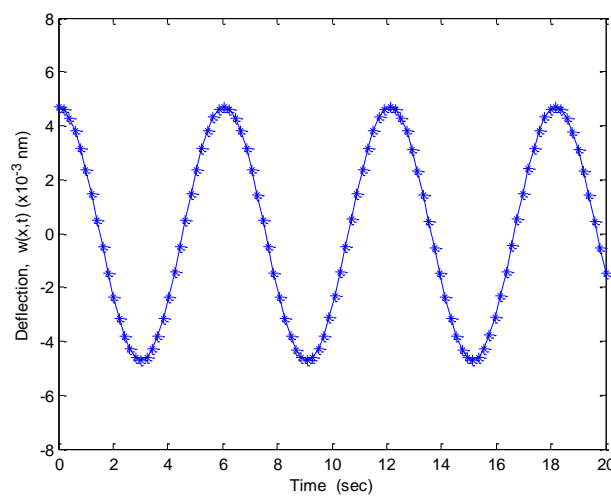

Figure 14. CNTs dynamic behaviour when Kn=0.03

The nonlocality (nonlocal parameter) is a scaling parameter which makes the small-scale effect to be accounted for in the analysis of microstructures and nanostructures.
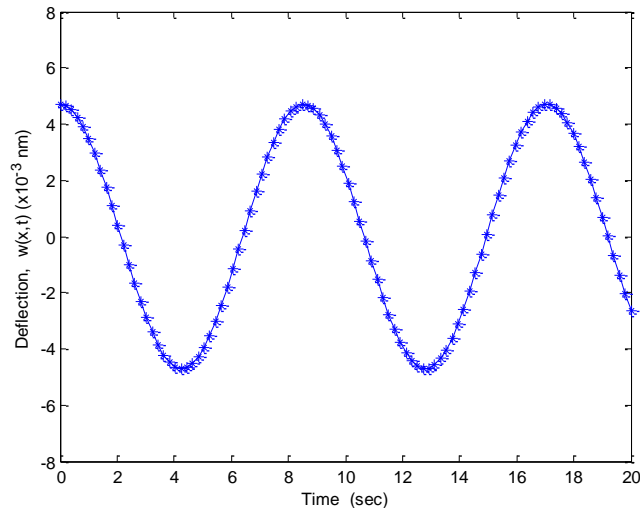
Figure 15. CNTs dynamic behaviour when Kn=0.05

Figure 7 depicts the effect of the nonlocality on the ratio of the frequencies reduces for varying adimensional amplitude. The fundamental frequency ratio of the CNTs reduces as the nonlocality is augmented. Also, the impact of the nonlocality on the ratio of the frequencies reduces as the amplitude of the structure is enhanced.

The variations in the ratio of the frequencies with adimensional nonlocal parameter for different temperature change are presented in Figures 8 and 9. In Figure 8, it is shown that an enhancement in temperature change at high temperature causes reduction in the ratio of the frequencies. However, at room or low temperature, the ratio of the frequencies of the nanostructure enhances as the temperature change enhances as shown in Figure 8. Also, the ratio of the frequencies at low temperatures is lower than at high temperatures.

The importance of magnetic field strength on the ratio of the frequencies of the nanotube is given in Figure 10. It is illustrated that the ratio of the frequencies reduces when the strength of the magnetic field enhances. Also, at high values of magnetic fields and amplitude of vibration, the discrepancy between the nonlinear and the linear frequencies is enhanced. A further investigation shows that the vibration of the CNTs approaches linear vibration when the magnetic force strength enhances to a certain high value. Such very high value of magnetic force strength which causes great attenuation in the beam can be adopted as a control and instability strategy for the nonlinear vibration system.

Figure 11 shows the comparison of the midpoint deflection of linear and nonlinear vibrations of the nanostructure. The nonlinear term causes stretching effect in the nonlinear in the nonlinear vibration. The significances of the nonlocal and slip parameters on the flow-induced dynamic responses of CNTs are analyzed in Figures 12-15. The enhancements of the nonlocal and slip parameters cause reduction in the vibration frequency and critical velocity.

CONCLUSION

In the current paper, the simultaneous impacts of surface elasticity, initial stress, residual surface tension and nonlocality on dynamic responses of CNTs carrying fluid while resting elastic foundations in a thermo-magnetic environment have been explored using methods of Galerkin decomposition and homotopy perturbation. The investigations showed that the positive and negative surface stress abates and improves the frequency ratio, respectively. The surface effect and frequency ratio are reduced as the length of the structure and nonlocality increase while the magnetic field strength and the nonlocal parameter decreases as the frequency ratio is increases. At a high temperature, the

frequency ratio is inversely proportional with the temperature change but directly proportional to the temperature change at room/low temperature. The present work will be very useful in the design and control of carbon nanotubes in thermo-magnetic environment while resting on elastic foundations.

Nomenclature

A   Area of the nanotube
E   Modulus of Elasticity
EI   bending rigidity
H_s residual surface stress
H_x magnetic field strength
I   moment of area
Kn   Knudsen number
L   length of the nanotube
m_c mass of tube per unit length
N   axial/Longitudinal force
T   change in temperature.
t   time coordinate
w   transverse displacement/deflection of the nanotube
W   time-dependent parameter
x   axial coordinate
$\phi(x)$ trial/comparison function
α_x coefficient of thermal expansion
η   magnetic field permeability
σ_v tangential moment accommodation coefficient

ACKNOWLEDGEMENTS

DECLARATION OF CONFLICTING INTERESTS

FUNDING

REFERENCES

[1]   S. Iijima, Nature, London, 354(1991), 56–58, 1991.
[2]   P. Abgrall and N. T. Nguyen, "Nanofluidic devices and their applications," Anal. Chem., vol. 80, pp. 2326–2341, 2008.
[3]   D. Zhao, Y. Liu, and Y. G. Tang, "Effects of magnetic field on size sensitivity of nonlinear vibration of embedded nanobeams," Mech. Adv. Mater. Struct., pp. 1–9, 2018.
[4]   A. Azrar, M. Ben Said, L. Azrar, and A. A. Aljinaidi, "Dynamic analysis of Carbon Nanotubes conveying fluid with uncertain parameters and random excitation," Mech. Adv. Mater. Struct., pp. 1–16, 2018.
[5]   V. Rashidi, H. R. Mirdamadi, and E. Shirani, "A novel model for vibrations of nanotubes conveying nanoflow," Comput. Mater. Sci., vol. 51, pp. 347–352, 2012.

[6] J. N. Reddy and S. Pang, "Nonlocal continuum theories of beams for the analysis of carbon nanotubes," J. Appl. Phys., vol. 103, pp. 023511, 2008.

[7] L. Wang, "A modified nonlocal beam model for vibration and stability of nanotubes conveying fluid," Physica E., vol. 44, pp. 25–28, 2011.

[8] C. W. Lim, "On the truth of nanoscale for nanobeams based on nonlocal elastic stress field theory: equilibrium, governing equation and static deflection," Appl. Math. Mech., vol. 31, pp. 37–54, 2010.

[9] C. W. Lim and Y. Yang, "New predictions of size-dependent nanoscale based on nonlocal elasticity for wave propagation in carbon nan- otubes," J. Comput. Theor. Nanoscience., vol. 7, pp. 988–995, 2010.

[10] R. Bahaadini and M. Hosseini, "Nonlocal divergence and flutter instability analysis of embedded fluid-conveying carbon nanotube under magnetic field," Microfluid. Nanofluid., vol. 20, pp. 108, 2016.

[11] M. Mahinzare, K. Mohammadi, M. Ghadiri, and A. Rajabpour, "Size-dependent effects on critical flow velocity of a SWCNT conveying viscous fluid based on nonlocal strain gradient cylindrical shell model," Microfluid. Nanofluid., vol. 21, pp. 123, 2017.

[12] R. Bahaadini and M. Hosseini, "Flow-induced and mechanical stability of cantilever carbon nanotubes subjected to an axial compressive load," Appl. Math. Modell., vol. 59, pp. 597–613, 2018.

[13] L. Wang, "Vibration analysis of fluid-conveying nanotubes with con-sideration of surface effects," Physica E., vol. 43, pp. 437–439, 2010.

[14] J. Zhang and S. A. Meguid, "Effect of surface energy on the dynamic response and instability of fluid-conveying nanobeams," Eur. J. Mech.-A/Solids., vol. 58, pp. 1–9, 2016.

[15] M. Hosseini, R. Bahaadini, and B. Jamali, "Nonlocal instability of cantilever piezoelectric carbon nanotubes by considering surface effects subjected to axial flow," J. Vib. Control., 2016.

[16] R. Bahaadini, M. Hosseini, and A. Jamalpoor, "Nonlocal and surface effects on the flutter instability of cantilevered nanotubes conveying fluid subjected to follower forces," Physica B., vol. 509, pp. 55–61, 2017.

[17] Wang GF, Feng XQ, Effects of surface elasticity and residual surface tension on the natural frequency of micro-beams. Journal of Applied Physics, 101, 013510, 2007.

[18] Wang GF, Feng XQ. Surface effects on buckling of nanowires under uniaxial compression. Appl Phys Lett 2009;94:141913-3, 2009.

[19] Farshi B, Assadi A, Alinia-ziazi A. Frequency analysis of nanotubes with consideration of surface effects. Appl Phys Lett, 96:093103–5, 2010.

[20] Lee HL, Chang WJ. Surface effects on axial buckling of non-uniform nanowires using non-local elasticity theory. Micro & Nano Letters, IET, 6(1): 19-21, 2011.

[21] Lee HL, Chang WJ. Surface effects on frequency analysis of nanotubes using nonlocal Timoshenko beam theory. J Appl Phys, 108:093503-3, 2010.

[22] Guo JG, Zhao YP. The size-dependent bending elastic properties of nanobeams with surface effects. Nanotechnology,18:295701–6, 2007.

[23] Feng XQ, Xia R, Li XD, Li B. Surface effects on the elastic modulus of nanoporous materials. Appl Phys Lett, 94:011913–6, 2009.

[24] He J, Lilley CM. Surface stress effect on bending resonance of nanowires with different boundary conditions. Appl Phys Lett 93:263103–8, 2008.

[25] He J, Lilley CM. Surface effect on the elastic behavior of static bending nanowires. Nano Lett, 8:1798–802, 2008.

[26] Jing GY, Duan HL, Sun XM, Zhang ZS, Xu J, Li YD, et al. Surface effects on elastic properties of silver nanowires: contact atomic-force microscopy. Phys Rev B, 73:235406–9, 2006.

[27] Sharm P, Ganti S, Bhate N. Effect of surfaces on the size-dependent elastic state of nano-inhomogeneities. Appl Phys Lett, 82:535–7, 2003.

[28] Wang ZQ, Zhao YP, Huang ZP. The effects of surface tension on the elastic properties of nano structures. Int J Eng Sci, 48:140–50, 2010.

[29] M. M. Selim, Vibrational analysis of carbon nanotubes under initial compression stresses , NANO Conference, April 5-7, 2009, King Saud University, KSA, 2009.

[30] H. Zhang and X. Wang, Effects of initial stress on transverse wave propagation in carbon nanotubes based on Timoshenko laminated beam models, Nanotechnoology 17, pp.45-53, 2006.

[31] X. Wang and H. Cai , Effects of initial stress on non-coaxial resonance of multi-wall carbon nanotubes, Acta Mater. 54, pp.2067–2074, 2006.

[32] K. Liu and C. Sun, Vibration of multi-walled carbon nanotubes with initial axial loading , Solid State Communications 143, pp. 202–207, 2007.

[33] X. Chen and X.Wang , Effects of initial stress on wave propagation in multi-walled carbon nanotubes Phys. Scr. 78, 015601 (9pp), 2008.

[34] M.M. Selim. Torsional vibration of carbon nanotubes under initial compression stress. Brazilian Journal of Physics, vol. 40, no. 3, 2010

[35] M.M. Selim. Vibrational Analysis of Initially Stressed Carbon Nanotubes. Vol. 119 ACTA PHYSICA POLONICA A No. 6, 2011.

[36] Selim MM. Vibrational analysis of initially stressed carbon nanotubes. Acta Phys Pol A.119(6):778–82, 2011.

[37] M, M. Selim and S. A. El-Safty Vibrational analysis of an irregular single-walled carbon nanotube incorporating initial stress effects. Nanotechnology Reviews 9: 1481–1490, 2020.

[38] Eringen, A.C.: Nonlocal polar elastic continua. Int. J. Eng. Sci. 10(1), 1–16, 1972.

[39] Eringen, A.C.: On differential equations of nonlocal elasticity and solutions of screw dislocation and surface waves. J. Appl. Phys. 54(9), 4703–4710, 1983.

[40] A. G. Arania, M. A. Roudbaria, S. Amir. Longitudinal magnetic field effect on wave propagation of fluid conveyed SWCNT using Knudsen number and surface considerations. Applied Mathematical Modelling 40, 2025–2038, 2016.

[41] R. Bahaadini and M. Hosseini, "Effects of nonlocal elasticity and slip condition on vibration and stability analysis of viscoelastic cantilever carbon nanotubes conveying fluid," Comput. Mater. Sci., vol. 114, pp. 151–159, 2016.

[42] M.G. Sobamowo, J.O. Akanmu, O.A. Adeleye, S.A. Akingbade, A.A. Yinusa. "Coupled effects of magnetic field, number of walls, geometric imperfection, temperature change, and boundary conditions on nonlocal nonlinear vibration of carbon nanotubes resting on elastic foundations. Forces in Mechanics, 3, 2021.

[43] J. H. He. Homotopy perturbation technique. Comput. Methods Appl. Mech. Eng. 178, 257-262, 2009.

[44] J. H. He. A coupling method of a homotopy technique and a perturbation technique for non-linear problems. Internat. J. Non- Linear Mech. 35, 37-43, 2000.

[45] J. H. He. Homotopy perturbation method: A new nonlinear analytical technique. Appl. Math. Comput. 135, 73-79, 2003.

[46] J. H. He. Some asymptotic methods for strongly nonlinear equation. Internat. J. Modern Phys. B. 20, 1144-1199, 2006.

[47] J. H. He. New interpretation of homotopy perturbation method. Internat. J. Modern Phys. B 20, 2561-2568, 2006.